Combining infrared and Raman spectra to assess MDI localization in novel flax-reinforced automotive composites

Sylvie Durand, Angélina d'Orlando, Laurent Mougnard, Alain Bourmaud, Johnny Beaugrand

Composites Part C: Open Access 12 (2023) 100382

Contents lists available at ScienceDirect

Composites Part C: Open Access

journal homepage: www.sciencedirect.com/journal/composites-part-c-open-access

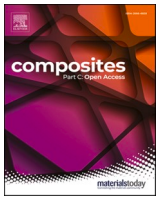

Combining infrared and Raman spectra to assess MDI localization in novel flax-reinforced automotive composites

Sylvie Durand [a,*], Angelina D'Orlando [a], Laurent Mougnard [b], Alain Bourmaud [c], Johnny Beaugrand [a]

[a] UR1268 Biopolymères Interactions Assemblages, INRAE, Nantes, France
[b] Howa-Tramico, Manufacturer, Brionne, France
[c] University Bretagne Sud, UMR CNRS 6027, IRDL, Lorient, France

ARTICLE INFO

Keywords:
FTIR
Raman
Flax fibres
Polyurethane
SEM

ABSTRACT

The present work describes the use of novel flax preforms reinforcement as substitution of glass fibres in complex composite stackings made of polyurethane foam impregnated with methylene diphenyl 4, 4′-diisocyanate (MDI), for automotive headliner parts manufacturing. Headliner structure, cohesion and mechanical performances are highly dependant of MDI distribution in both foam and fibre network. This study monitors the presence and localization of MDI in the final biobased composite by implementing a robust and innovative spectroscopic methodology. For that, Infrared and Raman spectroscopies are used to characterize the fibres and polymer chemical groups, such as the isocyanate and phenyl bonds in MDI and the urethane group. MDI in the flax preform is identified by the signal of the isocyanate group in the infrared spectrum. The complementary Raman study highlight two signatures of the interaction between polyurethane and MDI. One is the shift from 1620 to 1610 cm^{-1} between the urethane and the MDI aromatic vibration. The second is the aromatic ring substitution at 1530 cm^{-1}, which increases with the MDI concentration in the composite. These investigations demonstrate that MDI is present on the surfaces of flax fibres and foam and at the foam/fibre interfaces in the composite. The results clearly demonstrate the potential of flax for a use as headliner reinforcement, without penalizing the structure of the part.

Introduction

Before the 1970s, car headliner composites were constituted either of wood fibres coated by resin and waxes or styrene polycoated by paper. The use of these composite materials generated considerable noise and did not properly regulate environmental heat and moisture [1]. At the end of the 1970s, glass fibres were introduced into composites to improve the acoustic properties, and the addition of sprayed isocyanate significantly improved the thermal and moisture regulation ability. Innovative manufacturing processes and the development of polyethers, especially polyurethane foam, have resulted in the production of composites with enhanced mechanical properties, lower weights, and reasonable costs [2].

Typical headliner composites are composed of 7 to 9 layers, including several polymers (polyethylene, polypropylene, polyethylene terephthalate, and polyurethane) impregnated with MDI (methylene diphenyl 4,4′-diisocyanate) solution and amines as hardeners reinforced with glass fibres. These composite systems are well known to have suitable mechanical properties but the glass fibres have the main disadvantages of not being biodegradable or biobased and requiring a large quantity of energy for production. These effects could be mitigated by substituting synthetic or mineral fibres in composites by plant fibres (flax hemp, sisal, etc.), [3–6]. It is also useful to examine the patent literature: there are more than 150 international patents on headliners and their composition or manufacturing processes. The patents pending over the last 20 years show the development of multilayer composites, including natural fibres, as a result of end-user recommendations and internal standards [7–11].

Plants fibres (especially flax fibres) are of considerable interest in the composites field due to their availability (being mainly produced in France and other countries in Europe) and the existence of a strong value chain. They are mainly associated with the textile industry but are also developing for composite reinforcements, such as nonwoven, unidirectional or woven preforms [12]. These fibres exhibit unique mechanical

* Corresponding author.
E-mail address: sylvie.durand@inrae.fr (S. Durand).

https://doi.org/10.1016/j.jcomc.2023.100382

Available online 5 July 2023

Table 1
Samples and characterization. 'X' and '-' denote that the considered characterization technique was and was not performed on the sample, respectively.

References	Sample name	Origin	FTIR	Raman	SEM
MDI	MDI	Density 1.225 g/cm^{3,} Covestro Elastomer, Uerdingen, Germany	X	X	–
Polyurethane foam, (PU)	Foam 0	Ref E2024P, Howa-Tramico, Brionne, France	X	X	–
Flax fibres, 80 mm,	Flax 0	Eco-technilin, Valliquerville, France	X	X	X
Flax and MDI	Flax 0 + MDI	Howa-Tramico, Brionne, France	X	X	X
Car headliner Composites		Howa-Tramico, Brionne, France			
Flax and MDI	Flax 1	Flax in the composite 2	X	X	–
Flax and MDI	Flax 2	Flax in the composite 2	X	X	–
PU and MDI	Foam 1	Foam in Composite 1	X	X	–
PU and MDI	Foam 2	Foam in Composite 2	X	X	–
Composite	Foam 3	Foam in Composite 3	–	–	X

properties and are fully biobased and renewable with low environmental impact [13,14]. The environmental impact of the production of scutched flax fibres is approximately 8 times lower than that of E-glass fibres [13]. The use of biobased fibres opens up alternative end-of-life options, such as recycling and composting [15], that are not feasible for thermoset resins. Plant-fibre composites have a lower residue content after burning than that of glass-fibre composites and are therefore of interest in case of in incineration for heating or carbon production [16]; they can also be interesting for decreasing the knife degradation in case of grinding, compared to glass, much more abrasive. Polyurethane foam is synthesized by reacting isocyanates (TDI: toluene diisocyanate), polyol compounds and other additives. The polyols used are polyether (80 to 90% of the production) or polyesters, which are expensive and have a low resistance to hydrolysis but exhibit a high resistance to traction, flexion and abrasion [17]. The polymerized reaction products are polyurethane ester or polyurethane ether. MDI solution is added to reinforce adhesion between the fibres and foam, thereby stiffening the soft foam. A fundamental question in the fabrication of novel fibre-based car composites that may have industrial repercussions is whether MDI interacts differently with flax fibres than glass fibres.

Indeed, uncertainties remain about the behaviour of flax during the production process, especially concerning the localization of the MDI resin. To determine whether MDI can be absorbed by flax fibres, foam or at the fibre/foam interface, we designed a study on a composite of polyurethane foam reinforced by flax fibres impregnated with MDI resin.

The objective of this study was to develop a method for precisely identifying MDI in the final composite to assess the final quality of the parts. The use of flax preforms to reinforce composites made of polyurethane foam impregnated with MDI for use as headliner parts was carefully investigated.

First, Fourier Transform Infra-Red (FTIR) studies are carried out to obtain information about the principal chemical groups of each constituent of the composites. In addition, an in-depth Raman analysis is performed to thoroughly investigate the chemical structure of the layers and finally, SEM analysis is used to characterize the morphology of the flax fibres and the polyurethane foam at different scales. Principal Component Analysis is used to make connections amongst and confirm all the results.

Materials and methods

Materials

The flax fibres (*Linum usitatissimum*) used in this study were cultivated in Normandy in 2019 and field retted for 6 weeks. The retted flax stems were mechanically processed on an industrial scutching line (Depestele, Bourguebus, 14), and flax tows were collected and 80-mm cut for nonwoven manufacturing. The veil is an anisotropic preform with a machine direction orientation and an areal weight of 100 g/m^2.

This study was performed using reference sample consisting of MDI (density: 1.225 g/cm^3 Covestro Elastomer, Uerdingen, Germany) and polyurethane (PU) foam, 10-mm-thick, (E2024P) (Howa-Tramico, Brionne, France). Then, we analysed a mixed sample of flax fibres soaked with MDI and a composite of flax, MDI and PU foam (Table 1).

Fourier transform infrared spectroscopy

Spectroscopic investigations were already conducted to investigate the structure and arrangement of MDI components. Through FTIR analysis it is feasible to identify the isocyanate and phenyl groups in MDI and urethane groups [18–22]. FTIR is also a well know technique for identifying polysaccharides, and the alcohol and ester groups in the flax fibres [23–26].

In preparation for the FTIR analysis, approximately 1 g of each sample (Table 1) was cut with scissors, ground for 1 min at 20,000 rpm with an IKA 20 grinder and immersed in a liquid nitrogen cryogrinder (made of polycarbonate and stainless steel tube with a magnetic stirrer) for 8 min. FTIR spectra were recorded using potassium bromide (KBr, 120 mg) pellets containing 2 mg of each sample, with 5 repetitions per sample. The spectra were collected in transmission mode between 4000 and 400 cm^{-1} at a 2 cm^{-1} resolution with an IS50 spectrometer (ThermoFisher Scientific, Courtaboeuf, France). The infrared spectra were obtained from 200 coadded scans using OMNIC 9.2.41 software. All the spectra in the 2000–700 cm^{-1} region were baseline-corrected and unit-vector normalized using OPUS 7.5 software (Bruker Optics, France). The Unscrambler 10.1 software (CAMO, Oslo) was used to obtain the mean spectra and perform Principal Component Analyses (PCA). PCA is a multivariate analysis method for reducing a large number of data by creating linear combinations of uncorrelated variables [27] (Lebart et al., 1995). PCA determines the variability in sample data and extracts outlying data. PCA yields two plots: a score plot, which classifies the sample data into different groups with similar spectra, and a loading plot, which identifies the main wavenumber of each group (not shown).

Raman spectroscopy

Moreover, Raman microspectroscopy can reveal bonds that cannot be identified by infrared absorption [28,29]. As the isocyanate linkage in MDI also occurs in the polyurethane foam, Raman spectroscopy can be used to identify MDI by aromatic ring substitution [18,30,31].

Samples without preliminary preparation were observed on an aluminium slide, and Raman spectra were recorded using an InVia

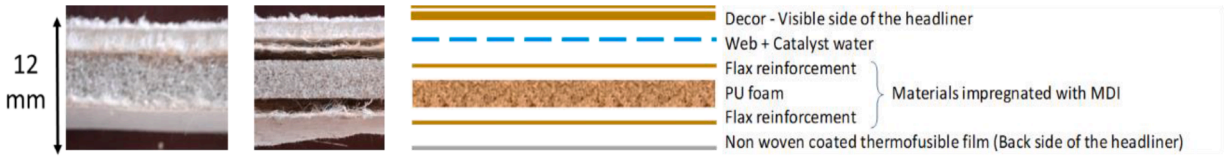

Fig. 1. Schematic of a stack of different layers in car headliner composites.

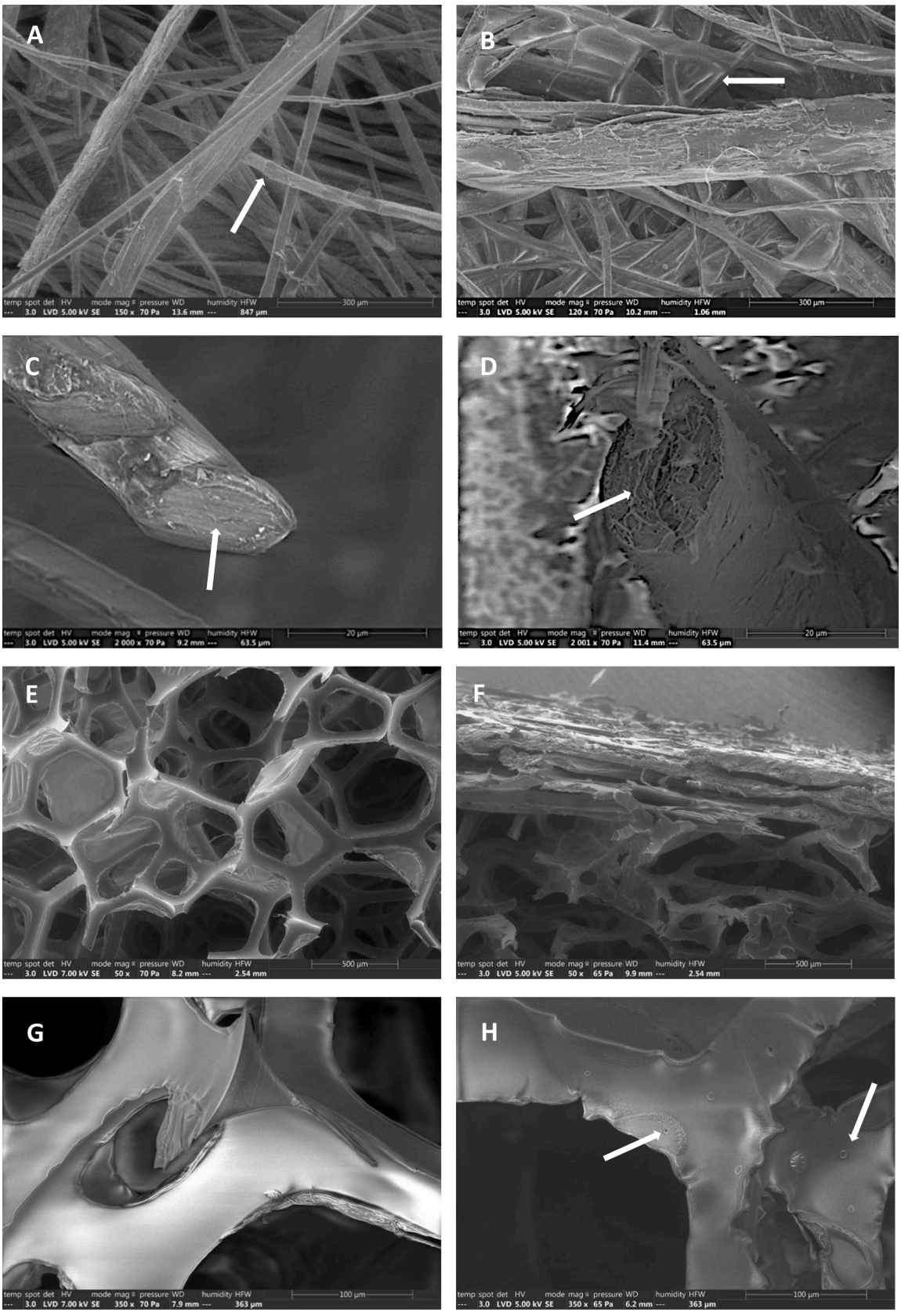

Fig. 2. SEM images of Flax 0 without MDI (A and C); Flax 0 with MDI (B and D); Foam 0 without MDI (E and G); and Foam 3 with MDI (F and H). The white arrows indicate specific characteristics of the samples.

Table 2
Assignments of the main bands in the FTIR spectra of flax fibers, MDI and polyurethane.

Wavenumbers (cm^{-1})	Assignments	Molecule	References
3200–3600	bound O—H	alcohol	Marechal and Chanzy, 2000
3300–3500	N-H amine	protein/ PU	Hiltz and al., 2001
2800–3000	CH_2, CH_3		Himmelsbach and al., 2002
2270	N = C = O	MDI	Pitsevitch and al., 2011 ; Boukrim and al., 2011
1720	C = O ester	MDI	Pitsevitch and al., 2011 ; Himmelsbach and al., 2002;
1705	bound C = 0	urethane	Hiltz and al, 2001 ; Colombini and al., 2008
1638	δ (OH) adsorbed water, C = O amide I	adsorbed water, protein	Himmelsbach and al., 2002; Marechal and Chanzy, 2000
1600	C = C aromatic	MDI	Pitsevitch and al., 2011
1540	C—N,N—H amide II	urethane	Hiltz and al, 2001 ; Colombini and al., 2008
1515	C = C aromatic	MDI/phenolic	Pitsevitch and al., 2011
1435	δ (CH) in CH_2	MDI	Pitsevitch and al., 2011
1245	δ (CH), δ (OH)	ester, acetyl	Himmelsbach and al., 2002
1225	ν (C—O-C)	urethane	Pelizzi, 2012; Hiltz and al., 2001
1167	ν (C—O-C) (asymmetric)	cellulose	Marechal and Chanzy, 2000
1135	ν (C—O-C) (ether)	MDI	
1105	ν (C—O)	cellulose	Marechal and Chanzy,
	ν (C-C), ν (C-H)	MDI	2000 ; Pitsevitch and al., 2011
1100	ν (C—O-C)	urethane	Hiltz and al., 2001
1062	ν (C—O) ν C—C	cellulose	Marechal and Chanzy, 2000; Beaugrand and al., 2022
1050	ν (C—O) ν C—C	mixture polysaccharide	Beaugrand and al., 2022
1028	ν (C—O) ν C—C	cellulose	Marechal and Chanzy, 2000; Beaugrand and al., 2022
895	ß (1–4) glycoside	cellulose	Marechal and Chanzy, 2000
815	δ CH aromatic	MDI	Hiltz and al., 2001
761	δ COO^-	MDI	Pitsevitch and al., 2011

confocal Raman microspectrometer (Renishaw, Marne la Vallée, France). Confocal Raman microscopy is a sensitive surface technique with a spatial resolution on the order of 250–500 nm. A 785-nm laser with a power of 100 mW was used with a grating of 1200 grooves/mm. The spectra were collected between 200 and 3200 cm^{-1} at a 1 cm^{-1} resolution using an X50 objective and a pinhole of 65 µm. Wire 4.2 software was used for data acquisition and processing to remove spikes and perform a baseline correction. Data smoothing, vectorial normalization, and spectral averaging were performed with The Unscrambler 10.1 software (CAMO, Oslo, Norway).

Scanning electronic microscopy (SEM)

Scanning Electron Microscopy (SEM) was performed using a QuattroS ESEM (ThermoScientific) microscope. Images were recorded using a low-vacuum detector to prevent sample deformation due to the use of high vacuum and without metallization. The acceleration voltage ranged from 3 to 7 kV, and the pressure ranged from 65 to 70 Pa. A cube of each sample was cut and taped on a copper support placed on the sample holder.

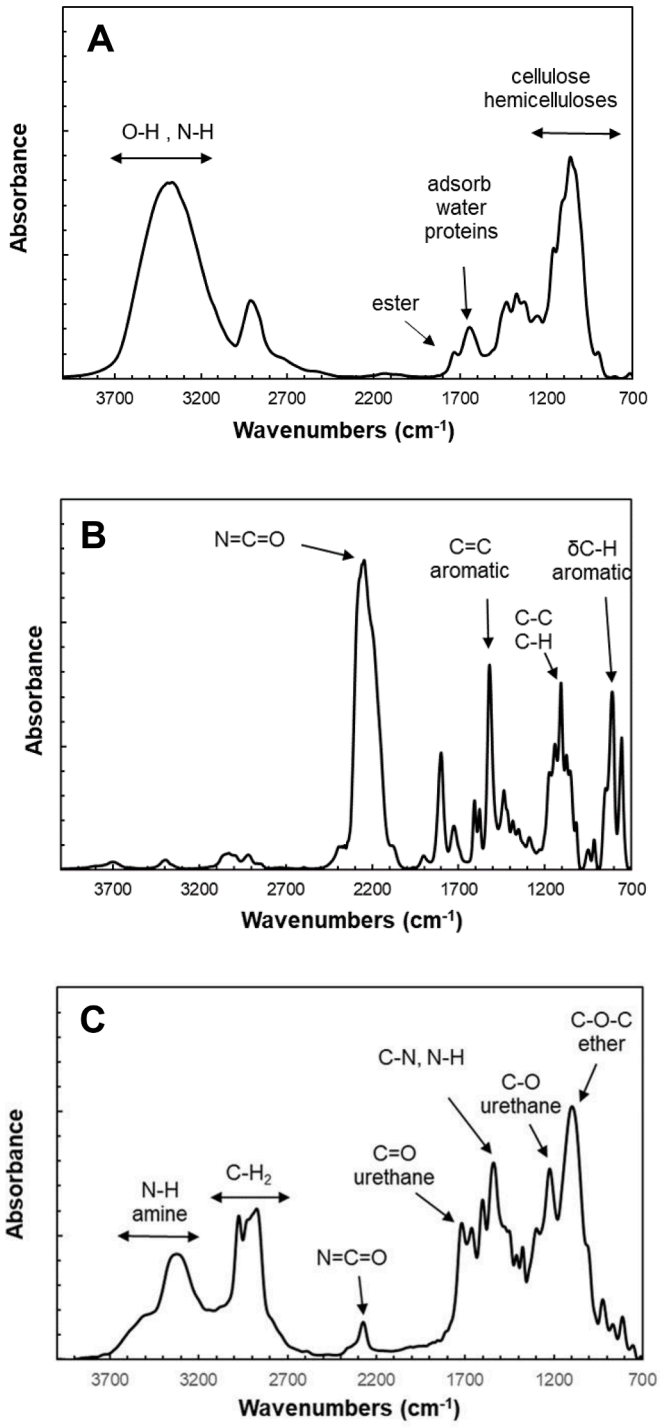

Fig. 3. FTIR spectra of Flax fibres (A), MDI solution (B), Polyurethane Foam (C).

Results and discussion

Morphological characteristics of samples

Scanning electron microscopy was used to observe the structural characteristics of the flax fibres and polyurethane foam components of the composite (Table 1 and Fig. 1) with and without MDI to analyse the impact of MDI on the fibre and foam surfaces and the fibre/foam interface (Fig. 2). The original foam has a homogeneous and smooth surface (Fig. 2. G, without MDI), whereas the foam soaked in MDI solution is no longer uniform, and small bubbles and discontinuities

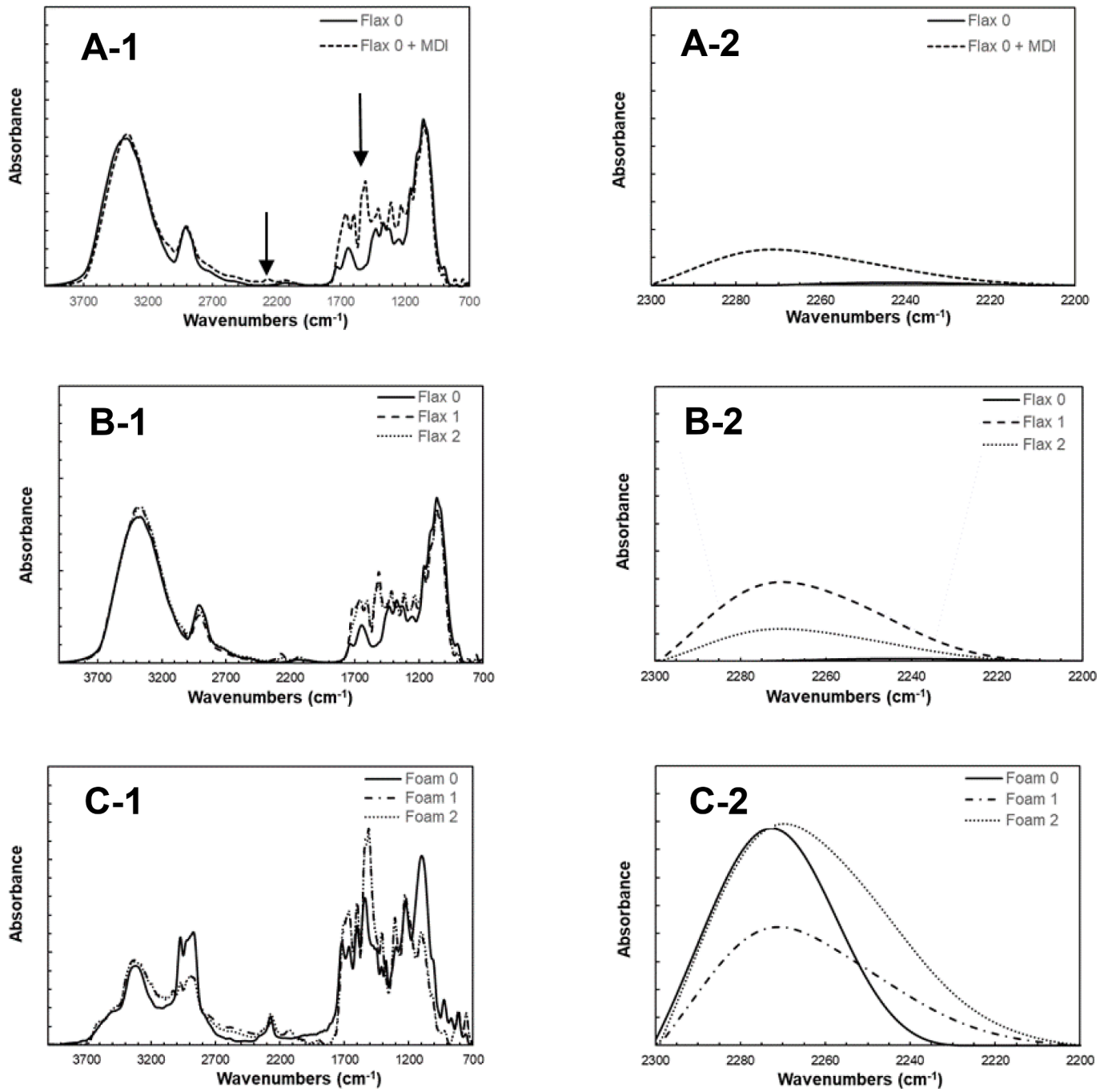

Fig. 4. FTIR spectra showing the 4000–700 cm^{-1} region (A. 1, B. 1, and C. 1) and magnification of the isocyanate peak at 2270 cm^{-1} (A. 2, B. 2, and C. 2): (A. 1 and A. 2) Flax 0 and Flax 0 + MDI; (B. 1and B. 2) Flax 0, Flax 1 in the composite + MDI and Flax 2 in the composite + MDI; and (C. 1 and C. 2) Foam 0, Foam + MDI in Composite 1 and Foam + MDI in Composite 2.

appear on the surface due to the presence of the MDI resin (Fig. 2. H, foam + MDI). MDI covers the flax fibres (Fig. 2. B and 2. D), and known defects kink bands [32], are no longer visible to the naked eye. A new matrix surrounds individual fibres, which is not observed for the flax fibres alone (Fig. 2. A, flax without MDI, 2. B, flax + MDI). MDI appears to have penetrated into the fibres, but this result cannot be confirmed by SEM observations. (Fig. 2. C, transverse section of flax without MDI and 2. D, transverse section of flax + MDI). Note that the embedment of the fibres in MDI may slightly reinforce and protect the fibres from tearing and collapsing during sample cutting.

FTIR analysis of reference samples with and without MDI

The flax fibre walls are mainly composed of cellulose, hemicelluloses, protein and lipids [33–36]. The main absorption bands and their assignments according to the literature are summarized in Table 2.

The 3800–3000 cm^{-1} region in the infrared spectra of the fibres (Fig. 3. A) exhibits hydrogen bonding vibrations associated with the ν(O—H) vibrations of alcohol and acid functional groups and the ν(N—H) vibrations of amine and amide functional groups [24]. Stretching vibration bands ν(N—H) appear from 3100 to 3500 cm^{-1}. The stretching vibration of bound water bands ν(OH) appear from 3200 to 3600 cm^{-1}.

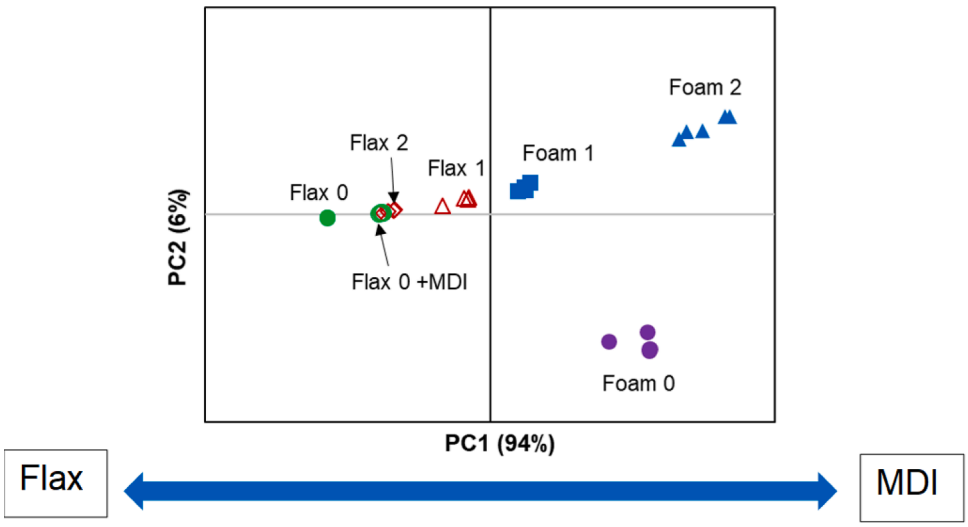

Fig. 5. Principal component analysis: the scatter plot of Components 1 and 2 for characterizing the sample in terms of the MDI concentration.

The bands at 1735 and 1245 cm^{-1} correspond to esters, whereas the absorption bands at approximately 1645 and 1540 cm^{-1} are characteristic of proteins. The 1640 cm^{-1} band could also correspond to internal water of the fibres [24,25].

Polysaccharides are usually characterized in the 1200–800 cm^{-1} spectral range. Cellulose, the major constituent of flax fibres, is identified by spectral bands at 898–995–1010–1030–1060–1105 and 1160 cm^{-1} [24]. The hemicelluloses, O-acetylated glucomannan, xylan and xyloglucan that are also present in flax fibre absorb in the same spectral region as cellulose but can be identified by the shoulder at approximately 940 and 815 cm^{-1} [34,37].

The MDI spectra (Fig. 3. B) are characterized by two important chemical groups: the isocyanate group N = C = O, which has a vibration at approximately 2270 cm^{-1} [18], and the phenyl group, which exhibits aromatic C = C stretching vibrations bands at approximately 1600 and 1515 cm^{-1} with an associated peak at 815 cm^{-1} corresponding to benzene C—H bending [21] and a -COO^{-} deformation band at approximately 760 cm^{-1} [18]. A peak for the isocyanate group is absent in the infrared spectra of the fibres alone and could therefore be a good indicator of the presence of MDI at the surface and/or interior of the fibres.

The infrared spectrum of polyurethane foam (Fig. 3. C) is dominated by urethane peaks: a ν(N—H) peak of the amine at approximately 3200 cm^{-1}, C=0 stretching vibration band at 1720 cm^{-1}, C—N and N—H stretching vibration band at 1540 cm^{-1} and C—O-C ether band at 1099 cm^{-1} [21]. These bands are accompanied by an aromatic skeletal vibration at approximately 1600 cm^{-1}, which is associated with a band at 815 cm^{-1} in response to out-of-plane C—H bending. The N=C=O stretching band of the isocyanate group at 2270 cm^{-1} [18] also appears in the spectrum, which reflects that the reaction between TDI and alcohol did not go to completion; this peak can be used as an indicator of the presence of MDI in the fibres but not in the polyurethane foam.

Flax-MDI

The infrared spectrum of flax fibres soaked in MDI solution is shown in Fig. 4. A. 1. The spectrum is clearly modified from that of the flax fibres due to the presence of MDI by the appearance of two main peaks: the N=C=O stretching band at 2270 cm^{-1} characteristic of the isocyanate group and the appearance of the phenyl C=C vibration at 1515 cm^{-1}. The isocyanate peak (Fig 4. A. 2) is a good indicator for use in sample classification. In the results presented below, we focus on the presence or absence of this isocyanate peak marker to analyse different composites.

FTIR – composites – ACP

The infrared spectra of composites containing flax fibres and MDI are shown in Fig. 4B. 1. The composites were prepared from two flax samples. The spectra are quite similar in the 4000–800 cm^{-1} region (Fig. 4. B. 1) but exhibit differences in the 2200–2100 cm^{-1} region (Fig. 4. B. 2). The difference in the peak intensities suggests that Flax 1 contains more MDI than Flax 2.

An analysis of the spectra of two polyurethane foams obtained from two composites (Fig. 4. C. 1) indicates that the presence of MDI results in a considerable increase in the intensity of the aromatic C = C vibration at 1515 cm^{-1} and a decrease in the intensity of the C—O-C ether vibration at 1100 cm^{-1} [18]. The 2270 cm^{-1} isocyanate vibration (Fig. 4. C. 2) appears in the spectra of the pure foam as well as in the spectra of both composites.

Principal Component Analysis (Fig. 5) was performed on the entire spectrum to grade the sample as a function of the intensity of the peak at 2270 cm^{-1} (loading PC1, not shown), which is correlated with the MDI concentration of the sample. The first component represents 94% of the total variability of the panel of the sample and separates the sample rich in fibres from the sample rich in MDI based on the intensity of the peak of the isocyanate N=C=O group.

Raman analysis of the foam reference sample and composite samples

We demonstrated in the first section that it is difficult to find MDI markers in polyurethane foam based on FTIR spectra alone. The isocyanate linkage in TDI, $N = O = C$, is present in polyurethane foam itself. Therefore, we use Raman spectra to identify more specific MDI markers, in particular, the ν(Aryl)-para disubstituted vibration of MDI in the vicinity of the 1530 cm^{-1} band, which does not appear in the FTIR spectrum [18,31].

The Raman spectrum of polyurethane (Fig. 6. A) is characterized by three main urethane peaks: the C = O stretching vibration at 1620 cm^{-1} and N—H stretching and C—H bending vibrations at 1450 and 1320 cm^{-1}, respectively.

The main peaks in the MDI spectrum (Fig. 6. B) are the C = C aromatic stretching vibration at 1610 cm^{-1}, the isocyanate linkage $N = O =$ C at 1445 cm^{-1}, and the para-disubstituted aromatic vibration at 1530 cm^{-1}. The main absorption bands and their assignments according to the literature are summarized in Table 3.

The spectra of the composite of polyurethane foam and MDI (Fig. 6. C) contains two peaks that correspond to the interaction between polyurethane and MDI. The first peak is the shift from 1620 to 1610

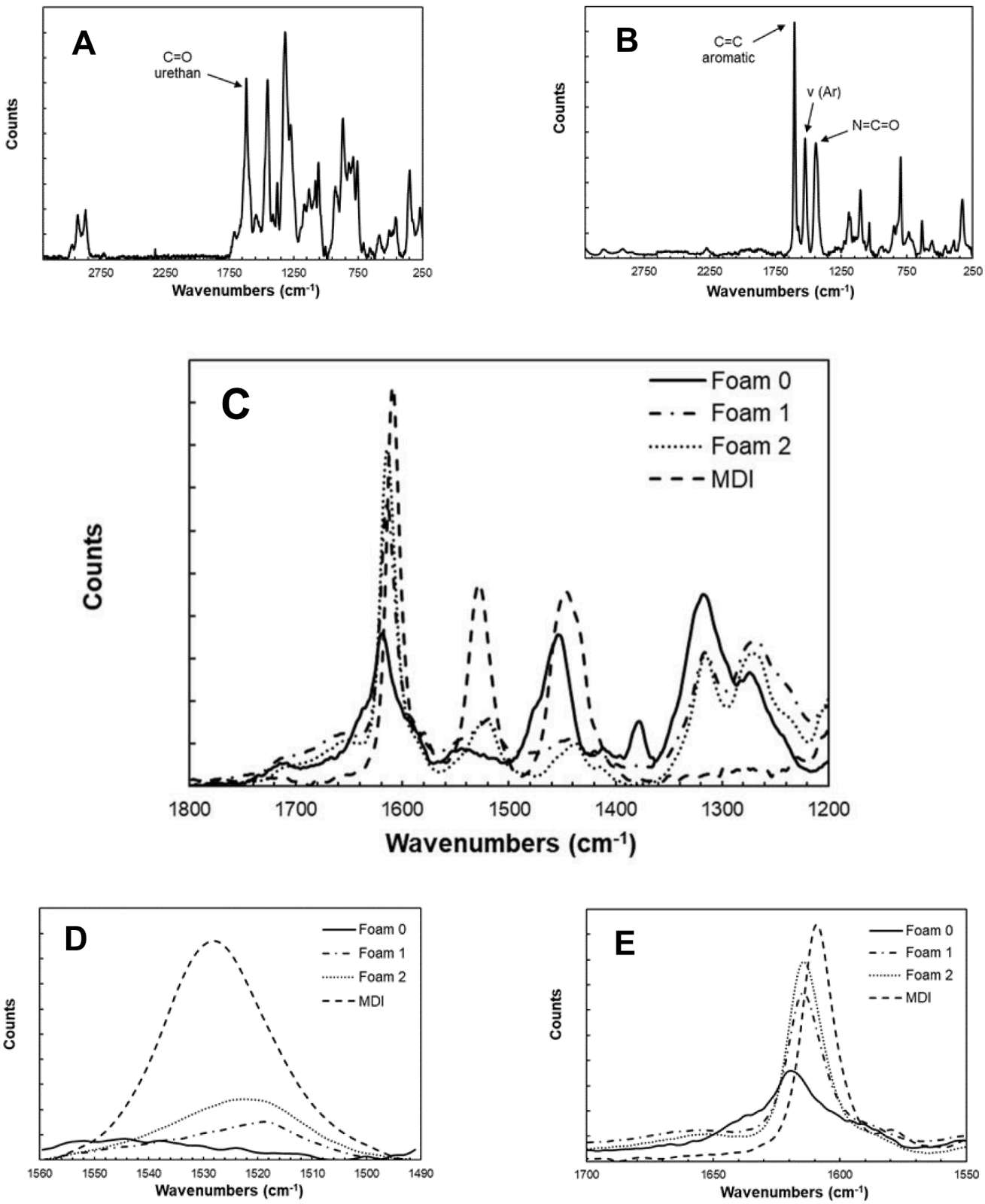

Fig. 6. Raman spectra: (A) Foam 0; (B) MDI solution; (C) Foam 0, Foam + MDI in Composite 1, Foam + MDI in Composite 2 and the MDI solution; (D) Shifts of C = O, C = C, Foam 0, Foam + MDI in Composite 1, Foam + MDI in Composite 2 and the MDI solution; and (E) the intensity of the peak at 1530 cm^{-1}: Foam 0, Foam + MDI in Composite 1, Foam + MDI in Composite 2 and the MDI solution.

Table 3
Assignments of the main bands in the Raman spectra of MDI and polyurethane.

Wavenumbers (cm^{-1})	Assignments	Molecule	References
1620	C = O	urethane	Weakley and al, 2012
1610	C = C aromatic,	MDI	Pitsevitch and al., 2011
1530	ν (ar) ; C—N and N—H in amide II	MDI/ urethane	Pitsevitch and al., 2011; Parnell and al., 2003
1445	ν N = C = O and ν (ar-N) δ CH_3 in -O-CH_3	MDI	Pitsevitch and al., 2011; Parnell and al., 2003
1314	C-H in amide III	urethane	Parnell and al., 2003
1105	ν C—C ar	MDI	Pitsevitch and al., 2011
800	δ C—H	MDI	Pitsevitch and al., 2011

cm^{-1} related to the C=O and/or the C=C aromatic vibration of urethane to the C=C aromatic vibration of the phenyl ring of MDI (Fig. 6. D). The second peak (Fig. 6. E) is the aromatic ring substitution at 1530 cm^{-1}, which increases with the MDI concentration of the composite.

Conclusions

Considering the application of the substitution of glass fibres with flax fibres in car headliner composite materials, we used complementary Raman and infrared spectroscopies to analyse the behaviour of MDI at the surfaces of flax fibres and foam or at the interfaces of different layers in automative composites. Raman spectroscopy clearly identified the interaction between the foam and MDI, and infrared measurements revealed the presence of MDI on the surfaces of the fibres. Our combined results demonstrate the potential of flax for a use as headliner reinforcement. Indeed, the tested headline panel is at the TRL 6, 7, meaning a prototype being demonstrated in a space environment, in respect with the stability and mechanical properties [6]. The threat was about the compatibility of the MDI, the main component in mass of the headliner, with the biogenic flax fibre reinforcement. In this study, tools for identification of the MDI on the contact of the flax non-woven net has been developed, and permit to conclude that the headliner structure is still cohesive albeit that the MDI distribution could varie in term of location, presence between fibre and layers. The use of the flax net for the fabric provide also a positive environmental foot print [14] and could be an economicaly interesting material regarding the initial E glass fibers used as reinforcement. Further studies are needed to conclude whether MDI soaks through to the middle of the fibres, which would require the use of a focused ion beam cutting tool to ablate the surface of the flax fibres. In addition, thin layers of composite need to be prepared to enable observation by SEM and infrared microspectroscopy or Raman microspectroscopy to determine the presence or absence of MDI inside the fibres.

Declaration of Competing Interest

The authors declare that they have no known competing financial interests or personal relationships that could have appeared to influence the work reported in this paper.

Data availability

Data will be made available on request.

Acknowledgments

The authors thank the BIBS instrumental platform for enabling us to carry out SEM experiments (http://www.bibs.inrae.fr/bibs_eng/, UR1268 BIA, IBiSA, PROBE infrastructure, Biogenouest). The authors also thank Fabienne Guillon (INRAE, BIA) for scientific support and sharing expertise on cell-wall components.

This study was funded by the INTERREG VA FCE Program, FLOWER Project, Grant Number 23.

References

[1] R.P. Doerer, M.D. Sandoe, A history of automotive headliners and characteristics of tramivex, an engineered composite material, SAE Tech. Pap. (1987), https://doi.org/10.4271/870381. Published online.
[2] Y. Araki, T. Suzuki, S. Hanatani, Composite material for automotive headliners - expandable stampable sheet with light weight and high stiffness, JFE Tech. Rep. 4 (4) (2004) 89–95.
[3] B.H. Lee, H.S. Kim, S. Lee, H.J. Kim, J.R. Dorgan, Bio-composites of kenaf fibers in polylactide: role of improved interfacial adhesion in the carding process, Compos. Sci. Technol. 69 (15–16) (2009) 2573–2579, https://doi.org/10.1016/j.compscitech.2009.07.015.
[4] Y. Chen, L. Sun, O. Chiparus, I. Negulescu, V. Yachmenev, M. Warnock, Kenaf/ramie composite for automotive headliner, J. Polym. Environ. 13 (2) (2005) 107–114, https://doi.org/10.1007/s10924-005-2942-z.
[5] A. Ashori, Wood-plastic composites as promising green-composites for automotive industries!, Bioresour. Technol. 99 (11) (2008) 4661–4667, https://doi.org/10.1016/j.biortech.2007.09.043.
[6] L. Mougnard, K. Behlouli, M. Haugel, J.B S.Durand, A. Kervoëlen, D. Shah, A. Bourmaud, Towards lightweight flax fibre-reinforced automotive headliners, JEC Compos. Mag. 147 (2022) 44–46.
[7] FR3001422A1, L. Rupert, L. Mougnard, L. Delbreilh, E. Dargent, Piece de garniture pour vehicules, comportant un panneau non tisse aiguillete pourvu de fibres naturelles vegetales et de fibres de polymere (2014).
[8] WO2016177960A1, C. Humbert, V. Bonin, L. Mougnard, Panel for covering and/or soundproofing a wall of a vehicle and associated method of manufacture (2016).
[9] WO2006112599A1, D.H. Seo,The member for interior products of motor vehicles with multilayer structure (2006).
[10] WO9902335A1, G. Gebreselassi, H.G. jr. Wolf, R. Michna Multilayer headliner with polyester fiber layer and natural fiber layers (1998).
[11] WO0006375A1, D.J. Shin, Laminated liner (1999).
[12] A. Bourmaud, J. Beaugrand, D.U. Shah, V. Placet, C. Baley, Towards the design of high-performance plant fibre composites, Prog. Mater. Sci. 97 (2018) 347–408, https://doi.org/10.1016/j.pmatsci.2018.05.005.
[13] A. Le Duigou, P. Davies, C. Baley, Environmental impact analysis of the production of flax fibres to be used as composite material reinforcement, J. Biobased Mater. Bio 5 (1) (2011) 153–165, https://doi.org/10.1166/jbmb.2011.1116.
[14] M. Gautreau, A. Kervoelen, G. Barteau, F. Delattre, T. Colinart, F. Pierre, M. Hauguel, N. Le Moigne, F. Guillon, A. Bourmaud, J. Beaugrand, Fibre individualisation and mechanical properties of a Flax-PLA non-woven composite following physical pre-treatments, Coatings 11 (846) (2021), https://doi.org/10.3390/coatings11070846.
[15] A. Melelli, D. Pantaloni, E. Balnois, et al., Investigations by AFM of ageing mechanisms in PLA-Flax fibre composites during garden composting, Polymers 13 (14) (2021), https://doi.org/10.3390/polym13142225 (Basel)2225.
[16] M.J. John, S. Thomas, Biofibres and biocomposites, Carbohydr. Polym. 71 (3) (2008) 343–364, https://doi.org/10.1016/j.carbpol.2007.05.040.
[17] E. Pellizzi, Étude du vieillissement des mousses de polyuréthane ester et consolidation par les aminoalkylalkoxysilanes, Published online (2012) 1–13. https://www.biblio.univ-evry.fr/theses/2012/2012EVRY0034.pdf.
[18] G.A. Pitsevich, M. Shundalau, M.A. Ksenofontov, D.S. Umreiko, Vibrational analysis of 4, 4 -methylene diphenyl diisocyanate, Glob. J. Anal. Chem. 2 (3) (2011) 114–124.
[19] A. Boukrim, Mousses de polyuréthane à l'eau, Published online (2011):110.
[20] A. Colombini, G. Corbin, V. Leal, Les matériaux en polyuréthanne dans les œuvres d'art : des fortunes diverses. Cas de la sculpture « Foot Soldier » de Kenji Yanobe, CeROArt (2) (2008) 0–15, https://doi.org/10.4000/ceroart.432.
[21] J.A. Hiltz, J.P. Szabo, FT-IR study of poly (ether) urethanes, 2001 Technical Report DREA-TM-2001-073.
[22] C. Wilhelm, J.L. Gardette, Infrared analysis of the photochemical behaviour of segmented polyurethanes: aliphatic poly(ether-urethane)s, Polymer 39 (24) (1998) 5973–5980, https://doi.org/10.1016/S0032-3861(97)10065-9 (Guildf).
[23] M. Gautreau, S. Durand, A. Paturel, S. Le gall, L. Foucat, X. Falourd, B. Novales, M. C. Ralet, S. Chevallier, A. Kervaloën, A. Bourmaud, F. Guillon, J. Beaugrand, Impact of cell wall non-cellulosic and cellulosic polymers on the mechanical properties of flax fibre bundles, Carbohydr. Polym. 291 (2022), 119599, https://doi.org/10.1016/j.carbpol.2022.119599.
[24] Y. Maréchal, H. Chanzy, The hydrogen bond network in I(β) cellulose as observed by infrared spectrometry, J. Mol. Struct. 523 (1–3) (2000) 183–196, https://doi.org/10.1016/S0022-2860(99)00389-0.
[25] D.S. Himmelsbach, D.E. Akin, Near-infrared fourier-transform raman spectroscopy of flax (Linum usitatissimum L.) stems, J. Agric. Food. Chem. 46 (3) (1998) 991–998, https://doi.org/10.1021/jf970656k.
[26] D. Stewart, G.J. McDougall, A. Baty, Fourier-transform infrared microspectroscopy of anatomically different cells of flax (*Linum usitatissimum*) stems during development, J. Agric. Food. Chem. 43 (7) (1995) 1853–1858, https://doi.org/10.1021/jf00055a019.
[27] L. Lebart, A. Morineau, M. Piron, Statistique Exploratoire Multidimensionnelle, Dunod, Paris, 1995, p. 439. ISBN 2-10-002886-3. Published online439.

[28] C. Barron, X. Rouau, FTIR and Raman signatures of wheat grain peripheral tissues, Cereal. Chem. 85 (5) (2008) 619–625, https://doi.org/10.1094/CCHEM-85-5-0619.
[29] N. Gierlinger, New insights into plant cell walls by vibrational microspectroscopy, Appl. Spectrosc. Rev. 53 (7) (2018) 517–551, https://doi.org/10.1080/05704928.2017.1363052.
[30] A.T. Weakley, T. Warwick, T.E. Bitterwolf, D.E. Aston, Multivariate analysis of micro-Raman spectra of thermoplastic polyurethane blends using principal component analysis and principal component regression, Appl. Spectrosc. 66 (11) (2012) 1269–1278, https://doi.org/10.1366/12-06588.
[31] S. Parnell, K. Min, M. Cakmak, Kinetic studies of polyurethane polymerization with Raman spectroscopy, Polymer 44 (18) (2003) 5137–5144, https://doi.org/10.1016/S0032-3861(03)00468-3 (Guildf).
[32] E. Richely, S. Durand, A. Melelli, A. Kao, A. Magueresse, H. Dhakal, T. Gorshkova, F. Callebert, A. Bourmaud, J. Beaugrand, S. Guessasma, Novel insight into the intricate shape of flax fibre lumen, Fibers 9 (4) (2021) 1–17, https://doi.org/10.3390/fib9040024.
[33] D.E. Akin, Linen most useful: perspectives on structure, chemistry, and enzymes for retting flax, ISRN Biotechnol. (2013) 1–23, https://doi.org/10.5402/2013/186534.
[34] D.S. Himmelsbach, S. Khalili, D.E. Akin, The use of FT-IR microspectroscopic mapping to study the effects of enzymatic retting of flax (*Linum usitatissimum L*) stems, J. Sci. Food. Agric. 82 (7) (2002) 685–696, https://doi.org/10.1002/jsfa.1090.
[35] E. Richely, A. Bourmaud, V. Placet, S. Guessasma, J. Beaugrand, A critical review of the ultrastructure, mechanics and modelling of flax fibres and their defects, Prog. Mater. Sci. (2022) 124, https://doi.org/10.1016/j.pmatsci.2021.100851.
[36] J. Beaugrand, C. Goudenhooft, C. Alvarado, et al., Evolution of the flax cell wall composition during development and after gravitropism by synchrotron fluorescence imaging, Ind. Crops Prod. 175 (2022) 1–39, https://doi.org/10.1016/j.indcrop.2021.114256.
[37] M. Kacuráková, P. Capek, V. Sasinková, N. Wellner, A. Ebringerová, FT-IR study of plant cell wall model compounds: pectic polysaccharides and hemicelluloses, Carbohydr. Polym. 43 (2) (2000) 195–203, https://doi.org/10.1016/S0144-8617(00)00151-X.